



CHARACTERIZATION OF THE SPHERICAL STABILIZATION FLOW REGIME BY TRANSIENT PRESSURE ANALYSIS

Freddy Humberto Escobar¹, Alfredo Ghisays-Ruiz² and Priyank Srivastav³

¹Universidad Surcolombiana/CENIGAA, Avenida Pastrana, Neiva, Huila, Colombia

²Universidad del Atlantico, Fac. de Ciencias Básicas, Antigua vía Puerto Colombia, Barranquilla, Atlántico, Colombia

³The University of Oklahoma, Mewborne School of Petroleum and Geological Engineering, E. Boyd St. SEC Rm, Norman, USA

E-Mail: fescobar@usco.edu.co

ABSTRACT

There are three typical cases in which a constant-pressure boundary is combined with some other transient periods giving origin to the formation of new flow regimes. Such cases are radial stabilization, linear stabilization and spherical stabilization. The first one when a radial flow regime finds a constant-pressure boundary, the late pressure derivative will display a straight line with a negative unit slope. Once all the boundaries have been felt by the transient wave the pressure derivative will take the classic cascade behavior. The third case takes place in elongated system when the well is near a lateral pressure-constant boundary, then a transient period is expected along the other side of the reservoir. A combination of that with the effect of the constant-pressure boundary leads to the formation of the linear stabilization or parabolic flow regime. The third case corresponds to a limited-entry well completed near a constant-pressure boundary. In that case a $-3/2$ slope is seen in the pressure derivative plot and no characterization of this has ever been presented in the literature. So, a governing equation for such flow regime is developed and characterization of that is achieved by both conventional analysis and the *TDS* technique so both vertical and horizontal permeabilities can be estimated. Synthetic examples were run to validate the applicability of the provided equations.

Keywords: spherical stabilization, vertical anisotropy, limited entry, partial penetration, partial completion, formation testing

1. INTRODUCTION

With the advent of newer technologies like wireline formation testing (WFT) tools for formation pressure testing, it is now possible to gain critical information about reservoir just after drilling of well. In many cases as shown by Frimann-Dahl *et al.* (1998) it has now become possible to replace the expensive drill stem tests which may take days to months with short duration formation pressure tests also called as Mini-Dst's, although these Mini-Dst's provide small radius of investigation as compared to normal well tests, nevertheless they can be analyzed using same well test analyses principles as illustrated by Daungkaew *et al.* (2004). In addition Daungkaew, S *et al* showed that WFT provides information about localized near wellbore phenomenon which may be masked in convectional well tests. While several probe configurations exists for conducting the test almost all WFT rely on inserting a probe in virgin reservoir and pumping reservoir fluids from probe for creating drawdown, accurate quartz gauges allows measurement of sand face pressure with time. Every WFT pressure data is expected to have spherical flow, Stewart and Wittmann (1979) introduced analytical solutions for analysis of spherical flow regime in WFT. If we want to extract maximum information from these tests, it becomes critically important to properly classify spherical flow and its transition to other regimes. In 1978, Tippie and Abbot showed that Analysis of pressure transient data in bottom water drive with partial

completion displays flow geometry that changes with time from spherical to hemispherical to linear flow depending on distance of perforations or position of probe in case of wireline formation tests with vertical reservoir boundaries. For this type of reservoir setting existing flow regimes does not adequately describe the flow system.

The radial stabilization flow regime has been taken into account by Escobar, Hernandez and Tiab (2010a) which using the intercept formed by the negative unit slope line and radial flow regime provided a way to estimate reservoir area. Regarding the linear stabilization much information has been produced. It was characterized by Escobar *et al.* (2004), Escobar *et al.* (2005a) and Escobar *et al.* (2005b). They plotted isobaric lines and find that these take the shape of a parabola. Then, they named parabolic flow. Before their recognition, Escobar *et al.* (2004) called it pseudo-hemispherical flow regime and provided some characterization to it. Later on, Escobar, Hernandez and Hernandez (2007b) provided the estimation of reservoir length, skin factor, well position and reservoir width with help of that flow regime. Even, a deeper characterization of skin factors in elongated systems was presented by Escobar and Montealegre (2006). The characterization of such regime in elongated systems with area anisotropy was conducted by Escobar, Tiab and Tovar (2007a) and a comprehensive study on elongated systems, including the parabolic fluid, is presented by Escobar (2008). Escobar, Hernandez and Saavedra (2010b) included the study of naturally fractured



elongated reservoirs. As far as transient rate analysis is concerned, the researches of Escobar, Rojas and Bonilla (2012a) Escobar Rojas and Cantillo (2012b) included the characterization of the parabolic flow regime.

No information was found for the characterization of the spherical stabilization flow regime which takes place in a limited-entry well completed near a constant-pressure boundary. A governing model for limited-entry wells with bottom constant-pressure boundary was presented by Ichara (1981) and a conventional analysis was introduced by Tippie and Abbot (1978) but they did not elaborate on the $-3/2$ slope.

This paper presents the recognition of a new flow regime for case of spherical flow under partial penetration where main hydrocarbon column is supported by bottom water drive or gas cap drive on top. This spherical partial penetration/Spherical stabilization flow regime have pressure derivative characteristic slope of $-3/2$ (although, since it is near boundary, it should be better called hemispherical stabilization) in contrast to $-1/2$ slope that is observed during normal spherical flow. This increase in slope can be envisioned as support provided by constant pressure boundary (gas cap or water drive) and thus development of this flow regime is dependent upon distance of perforation to boundaries as well as permeability anisotropy.

This paper also tries to demonstrate significance of newly found spherical partial penetration flow regime for estimation of permeability anisotropy of a reservoir system. This can provide us with an additional tool for estimation of reservoir permeability anisotropy where we do not have well defined spherical flow present in the pressure derivative diagnostic curves. Both *TDS* technique, Tiab (1993), and conventional analysis were implemented for the characterization of such regime. They were tested with synthetic examples.

2. MATHEMATICAL FORMULATION

2.1. Mathematical model

Ichara (1981) presented the solution for pressure behavior of a limited-entry well with a constant-pressure bottom boundary. The dimensionless time, pressure and pressure derivative used in this work are given as:

$$t_D = \frac{0.0002637kt}{\phi\mu c_r r_w^2} \quad (1)$$

$$P_D = \frac{kh\Delta P}{141.2q\mu B} \quad (2)$$

$$t_D * P_D' = \frac{kh(t * \Delta P')}{141.2q\mu B} \quad (3)$$

The vertical anisotropy or permeability ratio, I_v , is here defined as:

$$I_v = \frac{k_z}{k} \quad (4)$$

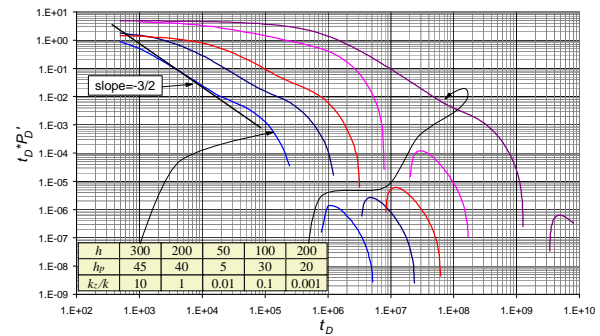


Figure-1. Dimensionless pressure derivative versus time log-log behavior for several values of reservoir thickness, perforated thickness and vertical/horizontal permeability ratio

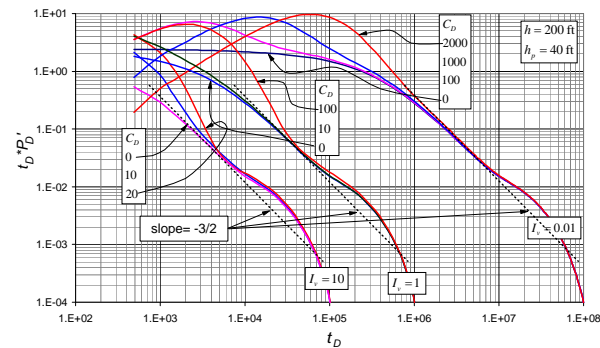


Figure-2. Effect of wellbore storage on the spherical stabilization flow regime.

And the penetration ratio, b , is defined as:

$$b = \frac{h_p}{h} \quad (5)$$

Spherical stabilization takes place when a partially completed well is perforated near a constant-pressure boundary, meaning that either there is a gas cap or a bottom aquifer overlying or underlying, respectively, the oil reservoir. This flow regime has a characteristic slope of $-3/2$ on the pressure derivative versus time log-log plot as seen in Figure-1. This flow regime can be seen if the formation is thick enough to provide its development. As seen in Figure-1 for reservoir thickness less than 50 ft. the spherical stabilization flow regime is not seen in spite



that a vertical/horizontal permeability ratio is small. Notice for the case of a smaller permeability ratio, last curve in the right, the spherical stabilization is seen for a reservoir thickness of 200 ft. Penetration ratios higher than 40 % avoids development of this flow regime. Notice that for low permeability contrast the radial flow is almost seen since the effect of the constant-pressure boundary is retarded. The complete steady-state period is fully developed once the transient wave has reached the no-flow pressure boundary; the thicker the reservoir the later the maximum point is seen. This maximum corresponds to both the presence of the no-flow boundary and the penetration ratio.

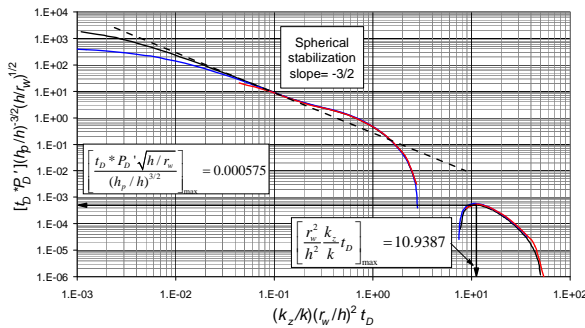


Figure-3. Unified behavior of the dimensionless pressure derivative versus time log-log.

Figure-2 is a dimensionless pressure derivative versus dimensionless time log-log plot for several values of dimensionless wellbore storage and anisotropy ratio. Spherical stabilization flow regime is affected more by wellbore storage for reservoir with higher anisotropy ratio. For instances when the anisotropy ratio is 10, meaning vertical permeability is 10 times higher than the horizontal permeability, dimensionless wellbore storage greater than 20 will mask the spherical stabilization flow regime. However, for the isotropic case the onset is at dimensionless wellbore storage of 100. Finally, when the permeability ratio is 0.01, dimensionless wellbore storage values up to 2000 allow seeing the spherical stabilization flow. Generally for reservoirs containing hydrocarbons due to geological sedimentary deposition horizontal permeability is greater than vertical permeability; hence, anisotropy ratio will be less than 1, therefore we expect to see spherical stabilization flow regime even for higher wellbore storage.

Figure-3 presents a unified pressure derivative curve for different values of reservoir thickness, thickness penetration ratio and vertical/horizontal permeability ratio. All the curves fall into a single one if the dimensionless time is multiplied by the permeability ratio and the pressure derivative is multiplied by the penetration ratio to the power -3/2. This allows developing the following mathematical model by regression analysis:

$$t_D * P_D' = \frac{\pi}{11} \sqrt{\frac{r_w}{h}} \left(\frac{1}{h_p} \frac{k_z}{k} \frac{r_w^2}{h} t_D \right)^{-3/2} \quad (6)$$

Integrating the above expression leads to:

$$P_D = -\frac{2\pi}{33} \sqrt{\frac{r_w}{h}} \left(\frac{1}{h_p} \frac{k_z}{k} \frac{r_w^2}{h} t_D \right)^{-3/2} + s_{sps} \quad (7)$$

The spherical stabilization skin factor, s_{sps} , is assumed to be a combination of the mechanical skin factor and the vertical flow.

2.2. TDS technique

This technique was introduced by Tiab (1995) and is based upon finding characteristic feature and points in the pressure and pressure derivative log-log plot. Replacing the dimensionless parameters given by Equations (1) and (3) into Equation (6) and solving for the radial permeability:

$$k = \frac{9417306.154 q \mu^{5/2} B \sqrt{r_w} \left(\frac{h_p \phi c_t}{k_z t_{sps}} \right)^{3/2}}{(t * \Delta P')_{sps}} \quad (8)$$

The pressure derivative $(t * \Delta P')_{sps}$ is read at any convenient time, t_{sps} , during the spherical stabilization flow regime. Equation (8) assumes that the value of the vertical permeability is known which may be obtained from a repeat wireline formation test. When the reservoir anisotropy as defined here is very low, see Figure-1, it is possible to see the radial flow regime. In such case, a horizontal line is drawn along the radial flow regime and the pressure derivative corresponding to such line is read and horizontal permeability can be obtained from the following expression developed by Tiab (1993):

$$k = \frac{70.6 q \mu B}{h (t * \Delta P')_r} \quad (9)$$

If this is the case, then, it is better to solve for the vertical permeability from Equation (8).

$$k_z = 44594.83 \left(\frac{q \mu^{5/3} B}{k (t * \Delta P')_{sps}} \right)^{2/3} \left(\frac{h_p \phi c_t}{t_{sps}} \right) \quad (10)$$

The spherical stabilization skin factor is obtained from the division of Equation (7) by Equation (8); then,



$$s = 66694.8h\sqrt{r_w} \left(\frac{h_p \phi \mu c_t}{k_z t_{sps}} \right) \left(\frac{\Delta P_{sps}}{(t^* \Delta P')_{sps}} + \frac{2}{3} \right) \quad (11)$$

Once horizontal permeability is calculated from Equation (8), the radial pressure derivative can be estimated from Equation (8), so:

$$(t^* \Delta P')_r = \frac{70.6q\mu B}{hk} \quad (12)$$

This value may be drawn as a horizontal line on the pressure derivative plot. This horizontal line takes the value of 0.5 in dimensionless form. Therefore, the intersection of the horizontal line with the spherical stabilization line allows obtaining the vertical permeability. The below equation is derived by setting the left-hand side of Equation (6) to 0.5 and solving for k_z :

$$k_z = \frac{2610.65h_p \phi \mu c_t r_w^{1/3} h^{2/3}}{t_{spsr}} \quad (13)$$

The normal case is that both vertical and horizontal permeabilities are unknown. In such case is when the TDS technique shows its power, capability and practicality. As observed in Figure-3, the coordinates of the maximum point are:

$$\left[\frac{t_D^* P_D' \sqrt{h/r_w}}{(h_p/h)^{3/2}} \right]_{\max} = 0.000575 \quad (14)$$

$$\left[\frac{r_w^2 k_z}{h^2 k} t_D \right]_{\max} = 10.9387 \quad (15)$$

When the dimensionless pressure derivative given by Equation (3) is replaced into Equation (14) and dimensionless time given by Equation (1) is plugged in Equation (15), it is possible to obtain expressions for estimating both horizontal and vertical permeabilities, respectively:

$$k = \frac{q\mu B h_p^{3/2} r_w^{1/2}}{12.3168h^3 (t^* \Delta P')_{\max}} \quad (16)$$

$$k_z = \frac{41481.608\phi\mu c_t h^2}{t_{\max}} \quad (17)$$

Notice that the second derivative is not used since the pressure derivative tendency is negative; then, the second derivative is going to be negative making impossible to plot on a log-log scale.

2.3. Conventional analysis

If the dimensionless quantities are replaced in Equation (6), it yields:

$$\Delta P = \frac{6278204.1q\mu^{5/2} B \sqrt{r_w} \left(\frac{h_p \phi c_t}{k_z} \right)^{3/2}}{k} t_{sps}^{-3/2} + \frac{141.2q\mu B}{kh} s_{sps} \quad (18)$$

Equation (18) suggests that a Cartesian plot of P_{wf} versus $t^{-3/2}$ for drawdown or of P_{wf} versus $(t_p + \Delta t)^{-3/2} + \Delta t^{-3/2}$ will provide a straight line which slope, m_{sps} , and intercept, b_{sps} , allow obtaining horizontal permeability (if k_z is known) and spherical stabilization skin, respectively;

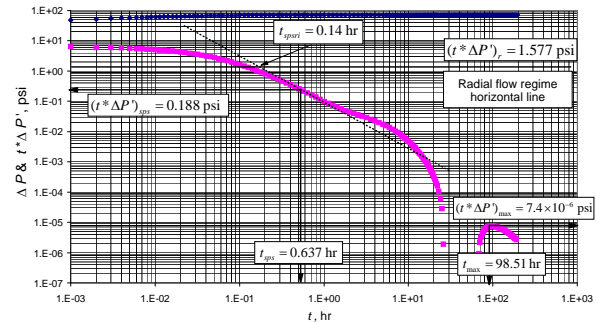


Figure-4. Pressure and pressure derivative versus time log-log plot for example 1.

$$k = \frac{6278204.1q\mu^{5/2} B \sqrt{r_w} \left(\frac{h_p \phi c_t}{k_z} \right)^{3/2}}{|m_{sps}|} \quad (19)$$

$$s_{sps} = \frac{k h b_{sps}}{141.2q\mu B} \quad (20)$$

As observed here, conventional analysis has a strong limitation if the vertical is unknown. In such case the best result from conventional analysis is to find the $k k_z^{3/2}$:

$$k k_z^{3/2} = \frac{6278204.1q\mu^{5/2} B \sqrt{r_w} (h_p \phi c_t)^{3/2}}{|m_{sps}|} \quad (19)$$



3. EXAMPLES

3.1. Synthetic example 1

A synthetic pressure test data was obtained with the information given below. Generated pressure drop and pressure derivative data are given in Figures-4 and 5, respectively.

- $B = 1.0$ bbl/STB
- $h = 200$ ft
- $r_w = 0.3$ ft
- $P_i = 5000$ psi
- $k = 50$ md
- $C_D = 0$
- $k_z = 5$ md
- $q = 200$ STB/D
- $\mu = 1$ cp
- $c_f = 3 \times 10^{-6}$ psi⁻¹
- $\phi = 10$ %
- $h_p = 40$ ft
- $s = 0$

Estimate horizontal and vertical permeabilities.

Solution by TDS technique

The following information was read from Figure-4:

$$t_{max} = 98.51 \text{ hr} \quad (t^* \Delta P')_{max} = 7.4 \times 10^{-6} \text{ psi}$$

$$t_{sps} = 0.637 \text{ hr} \quad (t^* \Delta P')_{sps} = 0.188 \text{ psi}$$

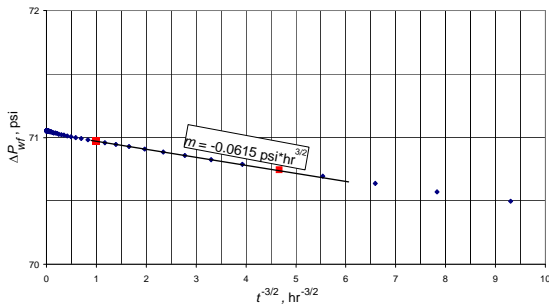


Figure-5. Pressure versus time to the power -3/2 for example 1.

Find horizontal permeability with Equation (16) using the maximum point pressure derivative:

$$k = \frac{200(1)(1)(40)^{3/2} \sqrt{0.3}}{12.3168(200)^3 (7.4 \times 10^{-6})} = 38 \text{ md}$$

Estimate the vertical permeability with Equation (17) using the time at which the maximum derivative occurs:

$$k_z = \frac{41481.608(0.1)(1)(3 \times 10^{-6})(200)^2}{98.51} = 5.05 \text{ md}$$

Use any arbitrary point on the spherical stabilization straight line and find permeability with Equation (8):

$$k = \frac{9417306.154(200)(1)^{5/2}(1)\sqrt{0.3}}{0.188} \left(\frac{(40)(0.1)(3 \times 10^{-6})}{(5.08)(0.637)} \right)^{3/2} = 39.5 \text{ m d}$$

Since permeability is known now, find with Equation (12) the value of the pressure derivative during radial flow regime masked by the effect of constant-pressure boundary:

$$(t^* \Delta P')_r = \frac{70.6(200)(1)(1)}{(200)(39.5)} = 1.7874 \text{ psi}$$

Now, draw a horizontal line going through 1.7874 psi, see Figure-4, and read the intersection of that line with the spherical stabilization straight line, extrapolated if needed,

$$t_{spsrsi} = 0.14 \text{ hr}$$

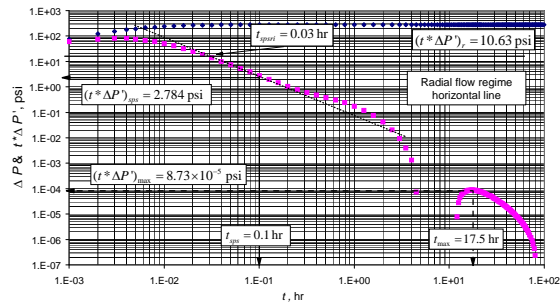


Figure-6. Pressure and pressure derivative versus time log-log plot for example 2.

Estimate again vertical permeability using Equation (13):

$$k_z = \frac{5.0627 \pi^{1.5} (40)(0.1)(3 \times 10^{-6})(0.3)^2}{200(1.55)} = 5.06 \text{ psi}$$

Solution by conventional analysis

A slope value of -0.0615 psi*hr^{3/2} was read from Figure-5. Assuming vertical permeability is known then horizontal permeability is estimated by means of Equation (19),

$$k = \frac{6278204.1(200)(1)^{5/2}(1)\sqrt{0.3}}{0.0615} \left(\frac{(40)(0.1)(3 \times 10^{-6})}{5} \right)^{3/2} = 40.94 \text{ m d}$$



3.2. Synthetic example 2

Another simulated example generated with the below information is reported in Figures-6 and 7. It is required to find the permeabilities from this test.

$$\begin{aligned}
 B &= 1.15 \text{ bbl/STB} & q &= 320 \text{ STB/D} \\
 h &= 120 \text{ ft} & \mu &= 3 \text{ cp} \\
 r_w &= 0.4 \text{ ft} & c_t &= 5 \times 10^{-5} \text{ psi}^{-1} \\
 P_i &= 3500 \text{ psi} & \phi &= 7 \% \\
 k &= 60 \text{ md} & h_p &= 30 \text{ ft} \\
 C_D &= 10 & s &= 0 \\
 k_z &= 72 \text{ md} & &
 \end{aligned}$$

Estimate horizontal and vertical permeabilities.

Solution by TDS technique

The following information was read from Figure-6:

$$\begin{aligned}
 t_{max} &= 17.5 \text{ hr} & (t^* \Delta P')_{max} &= 8.73 \times 10^{-5} \text{ psi} \\
 t_{sps} &= 0.1 \text{ hr} & (t^* \Delta P')_{sps} &= 2.784 \text{ psi}
 \end{aligned}$$

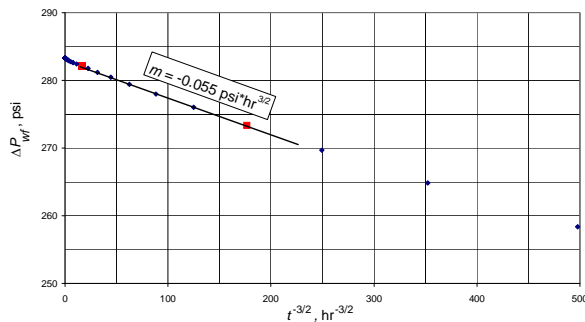


Figure-7. Pressure versus time to the power -3/2 for example 2.

As for the former example, Equation (16) is used to determine the horizontal permeability using the maximum point pressure derivative:

$$k = \frac{320(3)(1.15)(30)^{3/2} \sqrt{0.4}}{12.3168(120)^3 (8.73 \times 10^{-5})} = 61.75 \text{ md}$$

Now, using Equation (17) find the vertical permeability:

$$k_z = \frac{41481.608(0.07)(3)(1 \times 10^{-5})(120)^2}{17.5} = 71.7 \text{ md}$$

Verify the value of the horizontal permeability with Equation (8):

$$\begin{aligned}
 k &= \frac{9417306.154(320)(3)^{5/2}(1.15)\sqrt{0.4}}{2.784} \\
 &= \left(\frac{(30)(0.07)(1 \times 10^{-5})}{(71.7)(0.1)} \right)^{3/2} = 61.2 \text{ md}
 \end{aligned}$$

Any of the above horizontal permeability values, or an average, can be used to find $(t^* \Delta P')_r = 10.63$ psi from Equation (12). After drawing the horizontal line, the intersection point read is $t_{spsrsi} = 0.03$ hr which allows estimating again the vertical permeability using Equation (13);

$$\begin{aligned}
 k_z &= \frac{2610.65(30)(0.07)(3)(1 \times 10^{-5})(0.4)^{1/3}(120)^{2/3}}{0.03} \\
 k_z &= 72.4 \text{ md}
 \end{aligned}$$

Solution by conventional analysis

A slope value of $-0.055 \text{ psi} \cdot \text{hr}^{3/2}$ was estimated from Figure-7. Assuming vertical permeability is known then horizontal permeability is estimated using Equation (19),

Table-1. Summary of results from examples.

Example 1			
Parameter	Actual	TDS	Equation number
k , md	50	38	16
k , md	50	39.5	8
k_z , md	5	5.05	17
k_z , md	5	5.06	13
Parameter	Actual	Conventional analysis	Equation number
k , md	50	40.94	19
Example 2			
Parameter	Actual	TDS	Equation number
k , md	60	61.75	16
k , md	60	61.2	8
k_z , md	72	71.7	17
k_z , md	72	72.4	13
Parameter	Actual	Conventional analysis	Equation number
k , md	60	64.1	19



$$k = \frac{6278204.1(320)(3)^{5/2}(1.15)\sqrt{0.4}}{|-0.055|} \left(\frac{(30)(0.07)(1 \times 10^{-5})}{72} \right)^{3/2} = 64.1 \text{ md}$$

4. COMMENTS ON THE RESULTS

It is observed from Table-1 a good agreement between the actual and obtained results for both examples. Horizontal permeability estimated by either technique in the first example did not agree very much with the actual value, maybe, because it is a statistical model, but the vertical permeability results were excellent. In the second exercise both permeability provided a very good agreement with the actual data used for the simulation.

CONCLUSIONS

- Expressions for the characterization of the spherical stabilization flow regime were introduced and satisfactorily tested with synthetic examples. This regime can help in estimation of vertical permeability of reservoir.
- Spherical stabilization flow regime can prove very important for estimation of anisotropy ratio in analysis of pressure data obtained by wireline formation tester where pretest points are near constant pressure boundaries.
- For the *TDS* technique two equations for estimating horizontal permeability and two equations for estimating vertical permeability were introduced and tested. The permeability estimation does not depend on each other. For the case of conventional analysis one of the two permeabilities must be known to find the other one. This demonstrates the advantage and power of the *TDS* technique.

ACKNOWLEDGEMENTS

The authors thank Universidad Surcolombiana, Universidad del Atlántico and the University of Oklahoma for providing financial support for the completion of this study.

Nomenclature

B	Volume factor, rb/STB
B	Partial penetration ratio = h_p/h
C	Wellbore storage coefficient, bbl/psi
c_t	Total system compressibility, psi^{-1}
H	Reservoir thickness, ft
h_p	Perforated interval, ft
I_v	Vertical anisotropy, vertical to horizontal permeability ratio

K	Reservoir horizontal permeability, md
k_z	Reservoir vertical permeability, md
m_{sps}	Slope of the P . vs. $t^{3/2}$ plot
P	Pressure, psi
P_i	Initial reservoir pressure, psi
P_{wf}	Wellbore flowing pressure, psi
Q	Water flow rate, BPD
r_w	Wellbore radius, ft
S	Skin factor
T	Time, days
t_D	Dimensionless time coordinate
$t_D^*P_D'$	Dimensionless pressure derivative
$(t^*\Delta P')$	Pressure derivative

Greeks

ϕ	Porosity, fraction
μ	Viscosity, cp

Suffices

D	Dimensionless
i	Initial
max	Maximum before steady-state regime develops
r	Radial
sps	Spherical stabilization
$spsri$	Intercept of spherical stabilization and radial straight lines
wf	Well flowing
ws	Well static

REFERENCES

- Daungkaew S., Prosser D. J., Manescu A. and Morales M. 2004, January 1. An Illustration of the Information that can be obtained from Pressure Transient Analysis of Wireline Formation Test Data. Society of Petroleum Engineers. Doi: 10.2118/88560-MS.
- Escobar F.H., Saavedra N.F., Hernández C.M., Hernández Y.A., Pilataxi J.F. and Pinto D.A. 2004. Pressure and Pressure Derivative Analysis for Linear Homogeneous Reservoirs without Using Type-Curve Matching. Paper SPE 88874, Proceedings, 28th Annual SPE International Technical Conference and Exhibition to be held in Abuja, Nigeria, August 2-4.



- Escobar F.H., Muñoz O.F., Sepulveda J.A. Montealegre-M. M and Hernandez Y.A. 2005a. Parabolic Flow: A New Flow Regime Found In Long, Narrow Reservoirs. XI Congreso Colombiano del Petróleo (Colombian Petroleum Symposium). ISBN 958-33-8394-5. October 18-21.
- Escobar F.H., Muñoz O.F., Sepulveda J.A. and Montealegre M. 2005b. New Finding on Pressure Response In Long, Narrow Reservoirs. CT and F - Ciencia, Tecnología y Futuro. 2(6): 151-160. ISSN 0122-5383.
- Escobar F.H. and Montealegre-M. M. 2006. Effect of Well Stimulation on the Skin Factor in Elongated Reservoirs. CT and F - Ciencia, Tecnología y Futuro. 3(2): 109-119. ISSN 0122-5383.
- Escobar F.H., Tiab D. and Tovar L.V. 2007a. Determination of Areal Anisotropy from a single vertical Pressure Test and Geological Data in Elongated Reservoirs. Journal of Engineering and Applied Sciences. 2(11). ISSN 1816-949X. pp. 1627-1639.
- Escobar F.H., Hernández Y.A. and Hernández C.M. 2007b. Pressure Transient Analysis for Long Homogeneous Reservoirs using TDS Technique. Journal of Petroleum Science and Engineering. ISSN 0920-4105. 58(1-2): 68-82.
- Escobar F.H. 2008. Book "Petroleum Science Research Progress. Nova Publisher. ISBN 978-1-60456-012-1. 2008. Chapter "Recent Advances in Well Test Analysis for Long and Narrow Reservoirs.
- Escobar F.H., Hernandez Y.A. and Tiab D. 2010a. Determination of reservoir drainage area for constant-pressure systems using well test data. CT and F - Ciencia, Tecnología y Futuro. 4(1): 51-72. ISSN 0122-5383. June.
- Escobar F.H., Hernandez D.P. and Saavedra J.A. 2010b. Pressure and Pressure Derivative Analysis for Long Naturally Fractured Reservoirs Using the TDS Technique. Dyna, Year 77, Nro. 163, pp. 102-114. ISSN 0012-7353. September.
- Escobar F.H., Rojas M.M. and Bonilla L.F. 2012a. Transient-Rate Analysis for Long Homogeneous and Naturally Fractured Reservoir by the TDS Technique. Journal of Engineering and Applied Sciences. ISSN 1819-6608. 7(3): 353-370.
- Escobar F.H., Rojas M.M. and Cantillo J.H. 2012b. Straight-Line Conventional Transient Rate Analysis for Long Homogeneous and Heterogeneous Reservoirs. Dyna. Year 79, Nro. 172, pp. 153-163. ISSN 0012-7353. April.
- Frimann-Dahl C., Irvine-Fortescue J., Rokke E., Vik S. and Wahl O. 1998, January 1. Formation Testers vs. DST - The Cost Effective Use of Transient Analysis to Get Reservoir Parameters. Society of Petroleum Engineers. Doi: 10.2118/48962-MS
- Ichara M. J. 1981. January 1. Pressure Behavior in Vertically Fractured Wells Subject to Limited Entry and Bottom Water Drive. Society of Petroleum Engineers. Doi: 10.2118/10180-MS.
- Stewart G. and Wittmann M. 1979, January 1. Interpretation of the Pressure Response of the Repeat Formation Tester. Society of Petroleum Engineers. Doi: 10.2118/8362-MS.
- Tiab D. 1993. Analysis of Pressure and Pressure Derivative without Type-Curve Matching: 1- Skin and Wellbore Storage. Journal of Petroleum Science and Engineering. 12: 171-181. Also Paper SPE 25423 (1993) Production Operations Symposium held in Oklahoma City, OK.
- Tippie D. B. and Abbot W. A. 1978, January 1. Pressure Transient Analysis in Bottom Water Drive Reservoir with Partial Completion. Society of Petroleum Engineers. Doi:10.2118/7487-MS.